

CaM₂(PO₄)₂(HPO₄) (M = Fe or V): Phosphates containing Dimers of Edge-sharing MO₆ Octahedra*

Kwang-Hwa Lii

Institute of Chemistry, Academia Sinica, Taipei, Taiwan, Republic of China

Two new phosphates, CaM₂(PO₄)₂(HPO₄) (M = Fe^{III} or V^{III}), have been synthesised hydrothermally at 400 °C and characterized by single-crystal X-ray diffraction. Crystal data: CaFe₂(PO₄)₂(HPO₄), monoclinic, space group *P2₁/n*, *a* = 6.3663(6), *b* = 19.752(2), *c* = 6.5030(8) Å, β = 91.626(9)°, *Z* = 4 and *R* = 0.0240; CaV₂(PO₄)₂(HPO₄), as above except *a* = 6.359(2), *b* = 19.973(2), *c* = 6.4744(4) Å, β = 91.51(1)° and *R* = 0.0390. The two compounds are isostructural. The framework consists of corner-sharing PO₄ tetrahedra, HPO₄ groups and dimers of edge-sharing MO₆ octahedra forming M₂O₁₀ units. The structure of CaFe₂(PO₄)₂(HPO₄) was further defined by thermogravimetric and Mössbauer studies.

Several new compounds in the iron phosphate system have recently been synthesised and structurally characterized. The synthetic approaches were mainly hydrothermal methods. Hydrothermal synthesis involves the use of aqueous solvents or mineralizers under high temperature and high pressure to dissolve and recrystallize materials that are relatively insoluble under ordinary conditions. The iron phosphates that have been synthesised by the hydrothermal methods are AFeP₂O₇ (A = Cs or Rb),¹ Sr₂Fe(PO₄)₂(H₂PO₄),² SrFe₃(PO₄)₃(HPO₄),³ AFe₃(P₂O₇)₂ (A = Sr or Ba)⁴ and AFe₅(PO₄)₅(OH)·H₂O (A = Ca or Sr).⁵ They include iron(-III), (-II) and mixed-valence compounds. These phosphates are of interest for their complex network structures. They present a challenge to complete structural characterization from a basic research point of view. In addition, their study potentially allows for better understanding of the factors affecting their crystal structures. Attempts to add new members to the system have now yielded the iron(III) phosphate CaFe₂(PO₄)₂(HPO₄), the structure of which consists of dimers of edge-sharing FeO₆ octahedra, and the vanadium analogue CaV₂(PO₄)₂(HPO₄). This paper reports their hydrothermal synthesis and structural characterization.

Experimental

Synthesis.—Reagent-grade CaHPO₄·2H₂O, FePO₄, V₂O₅ and 85% H₃PO₄, obtained from Merck, were used as received. Crystals of CaFe₂(PO₄)₂(HPO₄) were grown by heating at 400 °C a mixture of CaHPO₄·2H₂O (0.1215 g), FePO₄ (0.2130 g) (molar ratio Ca:Fe = 1:2), and 3.75 mol dm⁻³ H₃PO₄ (2 cm³) in a sealed quartz glass tube (inside diameter 8 mm, outside diameter 10 mm) for 36 h followed by cooling to room temperature in 12 h. The glass tube was heated in a pressure vessel in which the pressure was balanced by an external pressure to keep the tube intact. Visual microscopic examination showed that the product contained many colourless crystals of CaFe₂(PO₄)₂(HPO₄) with some dark unidentified polycrystalline material. A single-phase product was not obtained, although several different reaction conditions were tested. Subsequently, a reaction was performed in a gold-lined Morey-type closure autoclave (17.5 cm × 3.3 cm inside diameter) with an internal volume of 140 cm³. A mixture of CaHPO₄·2H₂O (6.075 g), FePO₄ (10.65 g) (molar ratio

Ca:Fe = 1:2), and 3.75 mol dm⁻³ H₃PO₄ (70 cm³) was heated at 400 °C for 4 d followed by cooling to room temperature in 12 h. Upon opening the autoclave the product was found to contain many colourless crystals, several mm in length, and dark crystals of low quality. Energy-dispersive X-ray fluorescence analysis on a colourless crystal showed that the Ca:Fe:P mole ratio was 1:1.93:3.03. Powder X-ray diffraction analysis using a Rigaku powder diffractometer on a sample of manually selected colourless crystals compared well with that calculated from the single-crystal data. The composition was further characterized by thermogravimetric analysis under air using a DuPont thermal analyser. The sample began to decompose at ca. 600 °C and exhibited a weight loss of 1.95% at 900 °C. The weight loss corresponds to the loss of 0.5 water molecule and can be compared with the calculated value of 2.056%. The decomposition product was not characterized.

For the preparation of CaV₂(PO₄)₂(HPO₄), a mixture of CaHPO₄·2H₂O (1.200 g), V₂O₅ (1.046 g) (molar ratio Ca:V = 1:2), and 3.75 mol dm⁻³ H₃PO₄ (8 cm³) was heated at 400 °C in a smaller gold-lined Morey-type closure autoclave (5.2 cm × 2 cm inside diameter, internal volume 16 cm³) for 3 d and then cooled to room temperature in 12 h. The product contained green crystals of CaV₂(PO₄)₂(HPO₄) and dark crystals of low quality. An optimum reaction condition to reduce the amount of the side product was not found.

Single-crystal X-Ray Diffraction.—Crystals of dimensions 0.15 × 0.18 × 0.65 mm for CaFe₂(PO₄)₂(HPO₄) and 0.015 × 0.038 × 0.188 mm for CaV₂(PO₄)₂(HPO₄) were selected for indexing and intensity data collection on Nicolet R3m/V four-circle (for the iron compound) and Enraf-Nonius CAD4 diffractometers with κ-axis geometry (for the vanadium compound) using monochromated Mo-Kα radiation. The unit-cell parameters and orientation matrix were determined by least-squares fits of 32 peak maxima with 7 < 2θ < 28° and 25 with 12 < 2θ < 34° for the iron and vanadium compounds, respectively. Axial oscillation photographs were taken to check the unit-cell parameters and symmetry properties. Octants collected: ±*h*, +*k*, +*l* for both compounds. The intensity data for both crystals were corrected for Lorentz polarization and absorption effects. The latter were based on ψ scans of a few suitable reflections with χ values close to 90° using the program XEMP of the SHELXTL PLUS program package⁶ (for the iron compound) and the NRC VAX program package⁷ (for the vanadium compound). Based on systematic absences and successful solution and refinement of the structures, the space groups were determined to be *P2₁/n* for both compounds. This

* Supplementary data available: see Instructions for Authors, *J. Chem. Soc., Dalton Trans.*, 1994, Issue 1, pp. xxiii–xxviii.

non-standard space group was chosen so that the interaxial angle β was close to 90° . Direct methods were used to locate the metal atoms with the remaining non-hydrogen atoms being found from successive difference maps. Bond-strength calculations⁸ were carried out to help locate any hydrogen atoms. Atom O(2) was found to be undersaturated; sums of 1.48 and 1.44 valence units (v.u.s) were calculated for O(2) for the iron and vanadium compounds, respectively. All other oxygen atoms had valence sums close to 2.0. This suggested that a hydrogen atom is bonded to O(2), and it was located by scrutiny of a difference map. Both structures were refined by full-matrix least-squares refinement based on F values. For $\text{CaFe}_2(\text{PO}_4)_2(\text{HPO}_4)$, all of the non-hydrogen atoms were refined with anisotropic thermal parameters. For $\text{CaV}_2(\text{PO}_4)_2(\text{HPO}_4)$, anisotropic displacement parameter refinement was first attempted, but several oxygen atoms converged to non-positive-definite values, and therefore it was decided to remain in isotropic mode for the oxygen atoms. The atomic coordinates and isotropic thermal parameters for the hydrogen atoms were fixed. The multiplicities of the Ca atoms were allowed to vary but did not deviate significantly from full occupancy. Corrections for anomalous dispersion for both compounds and

secondary extinction for $\text{CaFe}_2(\text{PO}_4)_2(\text{HPO}_4)$ were made. Neutral-atom scattering factors were used. Structure determination and refinement were performed on DEC Micro VAX computer systems using the SHELXTL-PLUS program package.

Additional material available from the Cambridge Crystallographic Data Centre comprises H-atom coordinates, thermal parameters and remaining bond lengths and angles.

Mössbauer Spectroscopy.—The ^{57}Fe Mössbauer spectrum of $\text{CaFe}_2(\text{PO}_4)_2(\text{HPO}_4)$ was recorded at 300 K on a constant-acceleration type instrument. Velocity calibrations were made using 99.99% pure 10 μm iron foil. Typical linewidths for all three pairs of iron lines fell in the range 0.28–0.30 mm s^{-1} . Isomer shifts are reported with respect to iron foil at 300 K.

Results and Discussion

The crystallographic data for both compounds are listed in Table 1. The atomic coordinates, selected bond distances, and bond-valence sums are given in Tables 2 and 3. Both the Fe and V atoms are six-co-ordinated. The co-ordination number of Ca^{2+} was determined on the basis of the maximum gap in the Ca–O distances ranked in increasing order. In both compounds the calcium cation is co-ordinated by eight oxygen atoms and the ninth Ca–O bond length is ≈ 3.01 Å. Bond-valence sums for most atoms are in good accord with their formal oxidation states. In the following paragraphs only $\text{CaFe}_2(\text{PO}_4)_2(\text{HPO}_4)$ will be discussed because the two compounds are isostructural. Besides the two compounds, a few pairs of isostructural phosphates of Fe^{3+} and V^{3+} have also been synthesised. For example, $\text{Sr}_2\text{V}(\text{PO}_4)(\text{P}_2\text{O}_7)$,⁹ $\text{Ca}_2\text{V}(\text{PO}_4)(\text{HPO}_4)\cdot\text{H}_2\text{O}$,¹⁰ $\text{Sr}_2\text{V}(\text{PO}_4)_2(\text{H}_2\text{PO}_4)$,² $\text{Ba}_2\text{V}_3\text{H}(\text{PO}_4)_2(\text{P}_2\text{O}_7)_2$,¹¹ and AVP_2O_7 (A = alkali metal)¹² are isostructural with their iron analogues. The very similar ionic radii for V^{3+} and high-spin Fe^{3+} should account for this close structural correspondence.

As shown in Fig. 1, the framework of $\text{CaFe}_2(\text{PO}_4)_2(\text{HPO}_4)$ consists of Fe_2O_{10} units formed by two edge-sharing FeO_6 octahedra, phosphate tetrahedra, and hydrogenphosphate groups. Each octahedral edge-sharing dimer shares corners with three $\text{HP}(1)\text{O}_4$, four $\text{P}(2)\text{O}_4$, and three $\text{P}(3)\text{O}_4$ (Fig. 2). The oxygen atoms forming the shared edges are also shared by PO_4 tetrahedra. Dimers with the same orientation are linked through $\text{P}(2)\text{O}_4$ and $\text{P}(3)\text{O}_4$ tetrahedra, forming ribbons parallel to the c axis. Within a ribbon the disposition of Fe_2O_{10} units and phosphate tetrahedra is similar to that in $(\text{VO})_2\text{P}_2\text{O}_7$.¹³ Dimers in adjacent ribbons are oriented in a

Table 1 Crystal data and intensity collection parameters^a for $\text{CaFe}_2(\text{PO}_4)_2(\text{HPO}_4)$ and $\text{CaV}_2(\text{PO}_4)_2(\text{HPO}_4)$

Formula	$\text{CaFe}_2(\text{PO}_4)_2(\text{HPO}_4)$	$\text{CaV}_2(\text{PO}_4)_2(\text{HPO}_4)$
M	437.69	427.88
$a/\text{Å}$	6.3663(6)	6.359(2)
$b/\text{Å}$	19.752(2)	19.973(2)
$c/\text{Å}$	6.5030(8)	6.4744(4)
$\beta/^\circ$	91.626(9)	91.51(1)
$U/\text{Å}^3$	817.4(2)	822.1(2)
$D_c/\text{g cm}^{-3}$	3.556	3.457
$F(000)$	856	832
$\mu(\text{Mo-K}\alpha)/\text{cm}^{-1}$	48.4	35.6
Scan rate/ $^\circ \text{min}^{-1}$	2.93–14.65	5.49
Scan width/ $^\circ$	1.0 + $K\alpha$ separation	$0.70 + 0.35 \tan \theta$
Parameters refined	164	103
Reflections collected	2119	1947
Unique reflections [$I > 3\sigma(I)$]	1741	1212
g^b	0.000 516	0.000 464
R^c	0.0240	0.0390
R'^d	0.0299	0.0417

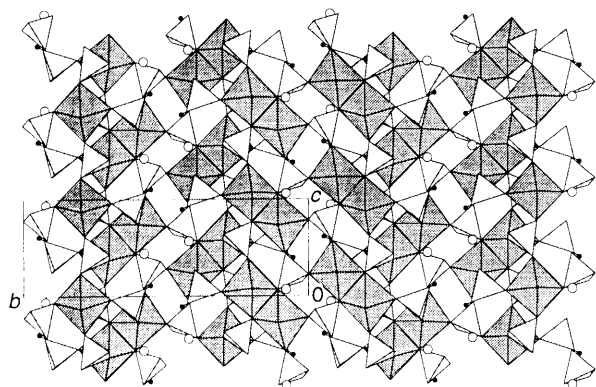
^a Details in common: monoclinic, space group $P2_1/n$; $Z = 4$; $T = 23^\circ\text{C}$; 2θ range 2–55°. ^b Weighting scheme of form $w^{-1} = \sigma^2(F) + gF^2$. ^c $R = \sum||F_o| - |F_c||/\sum|F_o|$. ^d $R' = [\sum w(|F_o| - |F_c|)^2/\sum wF_o^2]^{1/2}$.

Table 2 Atomic coordinates for $\text{CaFe}_2(\text{PO}_4)_2(\text{HPO}_4)$ and $\text{CaV}_2(\text{PO}_4)_2(\text{HPO}_4)$

Atom	X/a	Y/b	Z/c	X/a	Y/b	Z/c
$\text{CaFe}_2(\text{PO}_4)_2(\text{HPO}_4)$			$\text{CaV}_2(\text{PO}_4)_2(\text{HPO}_4)$			
Ca	0.643 4(1)	0.421 25(3)	0.437 9(1)	0.643 8(2)	0.420 41(7)	0.436 3(2)
M(1)	0.094 12(6)	0.402 87(2)	0.779 23(6)	0.097 6(2)	0.402 93(6)	0.765 8(2)
M(2)	0.058 48(7)	0.288 19(2)	0.403 60(7)	0.064 7(2)	0.289 71(5)	0.414 2(2)
P(1)	0.582 8(1)	0.379 40(4)	0.884 9(1)	0.586 1(3)	0.378 32(9)	0.883 0(2)
P(2)	0.057 3(1)	0.247 16(4)	0.911 4(1)	0.061 1(3)	0.248 33(9)	0.918 6(2)
P(3)	0.116 0(1)	0.448 44(4)	1.283 6(1)	0.118 9(3)	0.449 34(8)	1.281 7(2)
O(1)	0.786 3(3)	0.391 5(1)	0.775 1(3)	0.790 6(7)	0.393 2(2)	0.774 3(7)
O(2)	0.583 7(4)	0.427 6(1)	1.075 7(3)	0.579 2(8)	0.427 2(2)	1.074 3(7)
O(3)	0.403 6(3)	0.401 0(1)	0.736 2(3)	0.406 2(7)	0.399 8(2)	0.732 8(7)
O(4)	0.558 9(4)	0.307 9(1)	0.959 8(4)	0.567 4(8)	0.308 4(2)	0.956 7(7)
O(5)	0.090 7(3)	0.300 0(1)	0.735 8(3)	0.087 5(7)	0.300 2(2)	0.738 5(7)
O(6)	0.024 2(4)	0.285 6(1)	1.109 5(3)	0.038 9(8)	0.288 7(2)	1.114 8(7)
O(7)	−0.133 3(4)	0.200 8(1)	0.866 5(4)	−0.129 0(7)	0.202 7(2)	0.883 1(7)
O(8)	0.246 4(3)	0.199 3(1)	0.926 0(4)	0.252 7(7)	0.201 3(2)	0.927 4(7)
O(9)	0.138 6(4)	0.418 1(1)	1.068 9(3)	0.151 5(8)	0.419 6(2)	1.069 3(7)
O(10)	0.044 0(3)	0.391 6(1)	1.437 1(3)	0.045 5(7)	0.393 4(2)	1.436 6(6)
O(11)	0.323 6(3)	0.477 6(1)	1.362 0(3)	0.324 9(7)	0.478 8(2)	1.365 0(7)
O(12)	−0.065 9(3)	0.499 8(1)	1.282 8(3)	−0.064 7(7)	0.499 7(2)	1.277 9(7)

Table 3 Selected bond lengths (Å) and bond valence sums (Σs) for $\text{CaFe}_2(\text{PO}_4)_2(\text{HPO}_4)$ and $\text{CaV}_2(\text{PO}_4)_2(\text{HPO}_4)$ (in square brackets)

Ca–O(1)	2.423(2) [2.418(5)]	Ca–O(2)	2.378(2) [2.373(5)]
Ca–O(3)	2.535(2) [2.508(5)]	Ca–O(8)	2.473(2) [2.529(5)]
Ca–O(10)	2.618(2) [2.610(5)]	Ca–O(11)	2.390(2) [2.375(5)]
Ca–O(11)	2.359(2) [2.394(5)]	Ca–O(12)	2.637(2) [2.664(5)]
$\Sigma s(\text{Ca–O}) = 2.09$ [2.05]			
M(1)–O(1)	1.972(2) [1.964(5)]	M(1)–O(3)	1.998(2) [1.981(5)]
M(1)–O(5)	2.052(2) [2.060(5)]	M(1)–O(9)	1.921(2) [2.013(5)]
M(1)–O(10)	2.250(2) [2.157(4)]	M(1)–O(12)	1.972(2) [1.976(5)]
$\Sigma s[\text{M}(1)\text{–O}] = 3.01$ [2.84]			
M(2)–O(4)	1.933(2) [1.979(5)]	M(2)–O(5)	2.177(2) [2.111(4)]
M(2)–O(6)	1.919(2) [1.941(5)]	M(2)–O(7)	1.995(2) [1.969(5)]
M(2)–O(8)	2.011(2) [1.996(5)]	M(2)–O(10)	2.056(2) [2.081(5)]
$\Sigma s[\text{M}(2)\text{–O}] = 3.08$ [2.93]			
P(1)–O(1)	1.516(2) [1.524(5)]	P(1)–O(2)	1.564(2) [1.579(5)]
P(1)–O(3)	1.535(2) [1.542(5)]	P(1)–O(4)	1.503(2) [1.481(5)]
$\Sigma s[\text{P}(1)\text{–O}] = 5.08$ [5.06]			
P(2)–O(5)	1.565(2) [1.572(5)]	P(2)–O(6)	1.516(2) [1.515(5)]
P(2)–O(7)	1.541(2) [1.526(5)]	P(2)–O(8)	1.531(2) [1.539(5)]
$\Sigma s[\text{P}(2)\text{–O}] = 4.95$ [4.96]			
P(3)–O(9)	1.530(2) [1.518(5)]	P(3)–O(10)	1.579(2) [1.580(5)]
P(3)–O(11)	1.517(2) [1.522(5)]	P(3)–O(12)	1.539(2) [1.541(5)]
$\Sigma s[\text{P}(3)\text{–O}] = 4.92$ [4.93]			
O(2)–H	0.896 [1.036]	O(9)···H	2.124 [1.858]
O(11)···H	1.992 [1.967]		

**Fig. 1** View of the $\text{CaFe}_2(\text{PO}_4)_2(\text{HPO}_4)$ structure along the [100] direction. In this representation the corners of the octahedra and tetrahedra are O atoms and the Fe and P atoms are at the centre of each octahedron and tetrahedron, respectively. Small solid circles, H atoms; large open circles, Ca atoms

perpendicular direction. Adjacent ribbons are linked through $\text{HP}(1)\text{O}_4$ and $\text{P}(2)\text{O}_4$ to form a three-dimensional framework with channels running along the c axis (Fig. 3). The Ca atoms occupy sites in the walls of the channels. To my knowledge, this is the first time that discrete Fe_2O_{10} dimers have been found in iron(III) phosphates. In $\text{AFe}_3(\text{PO}_4)_5(\text{OH})\cdot\text{H}_2\text{O}$ ($A = \text{Ca}$ or Sr),⁵ dimers of edge-sharing FeO_6 octahedra can be recognized. Nevertheless, the Fe_2O_{10} units share edges with FeO_6 trigonal bipyramids. This is not the case for $\text{CaFe}_2(\text{PO}_4)_2(\text{HPO}_4)$ the Fe_2O_{10} units of which share corners with phosphate groups only. The V_2O_{10} units as observed in $\text{CaV}_2(\text{PO}_4)_2(\text{HPO}_4)$ are also rare. The compound $\text{KV}_4\text{P}_7\text{O}_{24}$ ¹⁴ is the only example of a structure built up from discrete V_2O_{10} units and phosphate groups. In the mixed-valence vanadium phosphate $\text{KV}_3\text{P}_4\text{O}_{16}$,¹⁵ dimers of edge-sharing VO_6 octahedra can also be

recognized, but they share corners to form infinite octahedral chains.

The ten vertices of each dimer in the present compound are shared by seven PO_4 groups and three HPO_4 groups. As shown by the $\text{O}\cdots\text{O}$ distances 2.666–3.193 Å for $\text{Fe}(1)\text{O}_6$ and 2.609–3.015 Å for $\text{Fe}(2)\text{O}_6$, both octahedra are strongly distorted. The length of the common edge of the two octahedra is 2.666 Å, considerably shorter than most of the edges which are not shared. The shortening of the shared edge is evidence that the structure is predominantly ionic. The iron atoms are displaced from the centroids of their FeO_6 octahedra away from each other such that the $\text{Fe}\cdots\text{Fe}$ separation is increased from 2.961 to 3.334 Å, indicative of the absence of iron–iron bonding. In $\text{CaV}_2(\text{PO}_4)_2(\text{HPO}_4)$ the $\text{V}\cdots\text{V}$ separation is increased from 2.964 to 3.211 Å. The average $\text{Fe}(1)\text{–O}$ and $\text{Fe}(2)\text{–O}$ distances are 2.027 and 2.015 Å, respectively. The *cis* O–Fe–O bond angles vary from 76.4 to 106.9° for $\text{Fe}(1)\text{O}_6$ and from 85.3 to 99.3° for $\text{Fe}(2)\text{O}_6$. The octahedral distortion can be estimated by using the equation $\Delta = (1/6)\Sigma[(R_i - \bar{R})/\bar{R}]^2$, where R_i = individual bond length and \bar{R} = average bond length.¹⁶ The results show that $\text{Fe}(1)\text{O}_6$ ($10^4\Delta = 27.8$) is more distorted than $\text{Fe}(2)\text{O}_6$ ($10^4\Delta = 18.1$). Atom $\text{Fe}(1)$ is coordinated by two HPO_4 groups in *trans* positions, $\text{Fe}(2)$ by one HPO_4 group. Each of the three unique phosphorus atoms is within a somewhat distorted tetrahedron. Atoms $\text{O}(5)$ and $\text{O}(10)$ are bonded to two iron atoms, and $\text{O}(2)$ to one H. Not surprisingly, the $\text{P}(1)\text{–O}(2)$, $\text{P}(2)\text{–O}(5)$ and $\text{P}(3)\text{–O}(10)$ distances are the longest P–O distances in the structure. Atoms $\text{O}(9)$ and $\text{O}(11)$ of a $\text{P}(3)\text{O}_4$ tetrahedron are hydrogen-bond acceptors from an adjacent $\text{HP}(1)\text{O}_4$ group.

Mössbauer Spectrum.—The room-temperature Mössbauer spectrum of $\text{CaFe}_2(\text{PO}_4)_2(\text{HPO}_4)$ (Fig. 4) was least-squares fit with two symmetric doublets of equal intensity. The parameters obtained are: δ (isomer shift) = 0.45 mm s^{-1} , ΔE_Q (quadrupole splitting) = 0.46 mm s^{-1} , and Γ (full width at half-height) = 0.38 and 0.35 mm s^{-1} for component 1; $\delta = 0.46$, $\Delta E_Q = 0.76$,

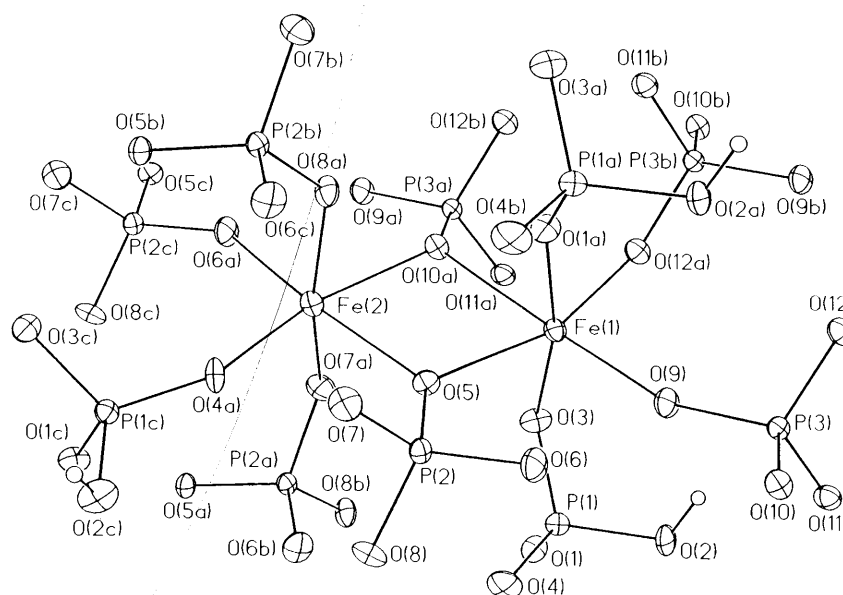


Fig. 2 The co-ordination of phosphate ligands around a dimer of edge-sharing FeO_6 octahedra in $\text{CaFe}_2(\text{PO}_4)_2(\text{HPO}_4)$

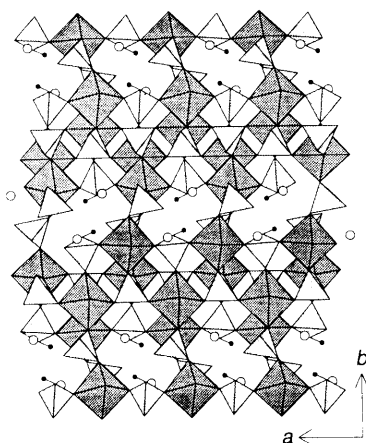


Fig. 3 View of the $\text{CaFe}_2(\text{PO}_4)_2(\text{HPO}_4)$ structure along the [001] direction

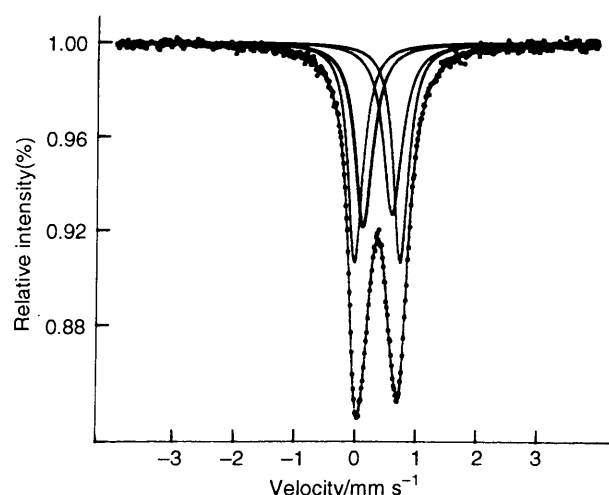


Fig. 4 Mössbauer spectrum of $\text{CaFe}_2(\text{PO}_4)_2(\text{HPO}_4)$ at 300 K

and $\Gamma = 0.30$ and 0.30 mm s^{-1} for component 2. The widths for the line at more positive velocity are listed first. The isomer shifts for both components are consistent with those for iron(III) phosphates as compiled by Gleitzer.¹⁷ Thus the Mössbauer spectrum confirms the presence of iron(III). Since a more

distorted octahedron is likely to have larger quadrupole splitting, component 2 can be assigned to Fe(1) and 1 to Fe(2).

Iron phosphates have shown a rich crystal chemistry owing to the accessibility of more than one iron oxidation state, the ability of iron to adopt different co-ordination geometries, and the great flexibility of iron-oxygen polyhedra. Further structural diversity is accomplished by introducing a variety of cations. The structures of the iron phosphates that have been characterized in this laboratory cover discrete FeO_6 octahedra, FeO_5 trigonal bipyramids, dimers of corner-, edge- and face-sharing FeO_6 octahedra, and infinite chains of FeO_6 octahedra sharing either *trans* or skew edges. Since hydrothermal methods have been successfully used in this system, it is likely that many more iron phosphates with novel frameworks will be forthcoming.

Acknowledgements

I thank Professor S. L. Wang at National Tsing Hua University, Dr. T. Y. Dong and Mr. Y. S. Wen at Academia Sinica for X-ray intensity data collection and Mössbauer spectroscopy measurements.

References

- 1 E. Dvoncova and K. H. Lii, *J. Solid State Chem.*, 1993, **105**, 279.
- 2 K. H. Lii, T. C. Lee, S. N. Liu and S. L. Wang, *J. Chem. Soc., Dalton Trans.*, 1993, 1051.
- 3 K. H. Lii, T. Y. Dong, C. C. Cheng and S. L. Wang, *J. Chem. Soc., Dalton Trans.*, 1993, 577.
- 4 K. H. Lii, P. F. Shih and T. M. Chen, *Inorg. Chem.*, 1993, **32**, 4373.
- 5 E. Dvoncova and K. H. Lii, *Inorg. Chem.*, 1993, **32**, 4368.
- 6 G. M. Sheldrick, SHELXTL-PLUS Crystallographic Systems, release 4.11, Siemens Analytical X-Ray Instruments, Madison, WI, 1990.
- 7 E. J. Gabe, Y. Le Page, J. P. Charland and F. L. Lee, *J. Appl. Crystallogr.*, 1989, **22**, 384.
- 8 I. D. Brown and D. Altermatt, *Acta Crystallogr., Sect. B*, 1985, **41**, 244.
- 9 T. C. Lee and K. H. Lii, unpublished work.
- 10 K. H. Lii, N. S. Wen, C. C. Su and B. R. Chueh, *Inorg. Chem.*, 1992, **31**, 439.
- 11 E. Dvoncova and K. H. Lii, *J. Solid State Chem.*, 1993, **106**, 485.
- 12 K. H. Lii, Y. P. Wang, Y. B. Chen and S. L. Wang, *J. Solid State Chem.*, 1990, **86**, 143; Y. P. Wang, K. H. Lii and S. L. Wang, *Acta Crystallogr., Sect. C*, 1989, **45**, 673; L. Benhamada, A. Grandin, M. M. Borel, A. Leclaire and B. Raveau, *Acta Crystallogr., Sect. C*,

- 1991, **47**, 424; K. H. Lii, unpublished work; Y. P. Wang and K. H. Lii, *Acta Crystallogr., Sect. C*, 1989, **45**, 1210.
- 13 Yu. E. Gorbunova and S. A. Linde, *Dokl. Akad. Nauk. SSSR*, 1979, **245**, 584.
- 14 L. Benhamada, A. Grandin, M. M. Borel, A. Leclaire and B. Raveau, *J. Solid State Chem.*, 1993, **104**, 193.
- 15 C. S. Lee and K. H. Lii, *J. Solid State Chem.*, 1991, **92**, 362.
- 16 R. D. Shannon, *Acta Crystallogr., Sect. A*, 1976, **32**, 751.
- 17 C. Gleitzer, *Eur. J. Solid State Inorg. Chem.*, 1991, **28**, 77.

Received 12th October 1993; Paper 3/06099C